Supporting Information

Designing porous and stable Au coating Ni nanosheets based Ni foam for quasi-symmetric polymer Li–air Batteries

Huimin Zhao, [a, ‡] *Xiaoqiang Liu,* [a, ‡] *Qingwei Zhang,* [a] *Huixiang Yin,* [a] *Zhirong Zhan,* [a] *Zhenzhen Chi,* [a] *Peilin Yang,* [a] *Zhenjiang Li,* [d] *Ziyang Guo, *,* [a,c] *and Lei Wang, *,* [a,b]

a. Key Laboratory of Eco-chemical Engineering, Taishan scholar advantage and characteristic discipline team of Eco chemical process and technology, College of Chemistry and Molecular Engineering, Qingdao University of Science and Technology, Qingdao 266042, P. R. China.

b. College of Environment and Safety Engineering, Qingdao University of Science and Technology, Qingdao, Shandong 266042, China.

c. Key Laboratory of Advanced Energy Materials Chemistry (Ministry of Education), College of Chemistry, Nankai University, Tianjin 300071, China

d. Qingdao Univ Sci & Technol, Coll Sinp German Sci & Technol, Qingdao 266061, Shandong, Peoples R China.

---

* Corresponding author. Tel & Fax: 0086-0532-84023409

E-mail address*: zyguo@qust.edu.cn; inorchemwl@126.com*

‡ Huimin Zhao and Xiaoqiang Liu contributed equally to this work.

Material Preparation

Materials

N-methyl-2-pyrrolidinone (C_5H_9NO, 99 %), Tetraethylene glycol dimethyl ether (TEGDME, 99.9 %) and Poly(methyl methacrylate) (PMMA) was purchased from Aladdin Reagent. 1.0 M bis (trifluoromethane) sulfonamide lithium salt (LiTFSI) in 1:1 v/v dimethoxyethane (DME) and 1, 3-dioxolane (DOL) with 2.0 wt% lithium nitrate ($LiNO_3$) additive 1 M $LiPF_6$ in 1:1 v/v ethylene carbonate (EC) and diethyl carbonate (DEC) solution were obtained from the Duoduo Reagent. Bis(trifluoromethane)sulfonimide lithium salt (LiTFSI) (Sigma-Aldrich, 99.95 %), $NiCl_2 \cdot 6H_2O$ (99.0 %) and $HAuCl_4$ (48~50% Au basis) was purchased from Macklin Reagent. Urea (AR) was purchased from Sinopharm Chemical Reagent Corp. NH_4F (98 %) was purchased from Aladdin Reagent. Carbon paper was TGP-H-060 carbon paper. Trimethylolpropane ethoxylate triacrylate (average Mn of ~428) and 2-hydroxy-2-methyl-1-phenyl-1-propanone ($C_6H_5COC(CH_3)_2OH$, 97%) were purchased from Sigma-Aldrich. Other chemicals were from All chemicals were used as received without further purification. Super P powders were purchased from Kejing Company.

The SP or Au/NNS-NF cathodes preparation

A mixture of Super P, and polyvinylidene fluoride (PVDF) binder with a weight ratio of 8:2 in N-methyl-2-pyrrolidone solvent was stirred to form homogeneous slurry. After that, the obtained slurry was spread on cabon paper via blade-coating to form the working SP electrode. Finally, the electrodes were dried at 100 °C for 24 h in an oven. The mass loadings of the active materials in the SP or Au/NNS-NF cathodes are generally 0.10-0.20 mg cm^{-2}.

Preparation of PMMA-based polymer electrolyte

1 M LiTFSI/TEGDME solution was denoted as Solution A. Then, Solution B containing PMMA/N-methyl-2-pyrrolidinone (NMP) (mass ratio: 1 : 4) was prepared. 2-hydroxy-2-methyl-1-phenyl-1-propanone(HMPP)/Trimethylolpropaneethoxylatetriacrylate (TMPET) (the mass ratio:

0.01 : 3) was also prepared and denoted as Solution C. The precursor solution was obtained by well mixing Solutions A, B, and C by the weight ratio of 4: 5: 3. Finally, the precursor solution was further irradiated under UV light (wavelength of 365 nm) for 20~35 s to form the PMMA-based polymer electrolyte (PMMA-PE).

Assembly of the symmetrical and Li–O_2/air batteries

All the batteries were assembled in an Ar-filled glove box with oxygen and water contents < 0.1 ppm: the cathode and anode were separated by the membranes filled with liquid electrolytes (the amount of the liquid organic electrolyte added in the Li–O_2 or symmetrical batteries is generally ~80 μL) or only PMMA-based polymer electrolyte (the content of the PMMA-based polymer electrolyte added in the conventional Li–air cells is usually around 150 μL) and then sealed into the battery configurations. For the symmetric batteries, both electrodes were Li@Au/NNS-NF, Li@NNS-NF or bare Li metal, and 1.0 M bis (trifluoromethane) sulfonamide lithium salt (LiTFSI) in 1:1 v/v dimethoxyethane (DME) and 1, 3-dioxolane (DOL) with 2.0 wt% lithium nitrate ($LiNO_3$) additive was used as electrolyte. For the Li–O_2 batteries, the cathodes were Au/NNS-NF or SP electrodes, the Li metals were applied as anode, and 1.0 M LiTFSI/tetraglyme (TEGDME) was used as electrolyte, respectively. Moreover, for the quasi-symmetric polymer Li–air batteries, the cathode was also Au/NNS-NF electrode, but their anodes and electrolyte were the Li@Au/NNS-NF electrodes and the PMMA-based polymer electrolyte, respectively. All the electrochemical performance tests were performed by the LAND battery test system (Wuhan Land Electronic Co. Ltd).

Ion Conductivity tests

Electrochemical impedance spectroscopy of PMMA-based polymer electrolyte or liquid electrolyte in the frequency ranging from 0.01 Hz to 100 kHz using symmetric cell (SSS/electrolyte/SSS). The tested electrolyte resistance is obtained from the intercept of the Nyquist plot with the real axis. The conductivity σ of the prepared electrolyte membranes are obtained using the following equation:

$$\sigma = l/RS$$

Here, R is the measured resistance of the prepared electrolyte, l is the thickness of the prepared electrolyte membrane between counter SSS electrodes, and S is the contact area of the prepared electrolyte membrane and the electrodes.

In situ DEMS tests

To investigate the gas evolution of the Au/NNS-NF based Li–air battery, the *in situ* DEMS measurement has been conducted. Firstly, an Au/NNS-NF cathode and a Li anode which are separated by the Celegard membrane are assembled into a customized Swagelok cell in an Ar-filled glovebox (water and oxygen below 0.01 ppm). Then, the DEMS cell was transferred out of the glovebox. Then, the Au/NNS-NF based customized Swagelok battery (there are two tubes on the top of the battery which act as the gas inlet and outlet) was transferred out of the glovebox and subsequently connected with the leak inlet of a differential electrochemical mass spectrometer (DEMS, Prisma Plus). After that, the above DEMS system was used to record the gas variation over recharge. Before testing, the Au/NNS-NF based DEMS battery was firstly discharged in the ambient air at 0.3 mA. Subsequently, the above DEMS cell was further treated with the carrier gas (pure Ar) to remove the residual O_2/CO_2 gas and ensure the corresponding baseline stability. After 10 hours, the above DEMS battery was persistently recharged at 0.3 mA for 2 hours and the corresponding gas evolution was also recorded by the DEMS device at the same time.

The fabrication of the quasi-symmetric polymer Li–air soft package cell

Li@Au/NNS-NF belt is obtained by rolling the Li@Au/NNS-NF film. Then Li@Au/NNS-NF belt was used as inner anode. Then the precursor solution of the

PMMA-PE was coated on the surface of Li@Au/NNS-NF and subsequently treated by UV irradiation for ~60 s. Then, the cathode was enwound on the surface of PMMA-PE coated Li@Au/NNS-NF anode. Finally, the above flexible Li–air battery was sealed into a soft bag. All the mentioned batteries were assembled in the pure Ar-filled glove box with O_2 and H_2O contents < 0.1 ppm. In addition, all the cells were cycled in the eight-channel LAND battery test system.

Detection of PMMA or PVDF reacted with O_2^- via FT-IR technology

In a typical experiment, 30 mg PMMA was reacted with 2 mL TEGDME with 0.1 M KO_2 + 0.3 M 18-crown-6 for 24 h. The resultant solid product, which was collected from the above solution, was further washed with DME for several times and dried under vacuum at room temperature for 10 hours. Next, the obtained samples and pure PMMA were directly detected by FT-IR technology. The PVDF samples before and after reaction were detected under same condition.

Characterization instrumentation

XRD measurements were performed on a Bruker D8 Focus power X-ray diffractometer with Cu K□ radiation. Field emission scanning electron microscopy SEM investigations were conducted using a JSM-6390 microscope from JEOL. Transmission electron microscopy (TEM) experiments were using a JEOL 2011 microscope (Japan) operated at 200 kV. Fourier transform-infrared spectroscopy (FT-IR) tests were performed on a Nicolet 6700 spectrometer. X-ray photoelectron spectroscopy (XPS) was conducted with a Thermo Escalab 250 equipped with a hemispherical analyzer and using an aluminum anode as a source. LAND cycler (Wuhan Land Electronic Co. Ltd) was employed for electrochemical tests. EIS experiments and electrodeposition experiments were conducted on an electrochemical workstation (CHI 760E).

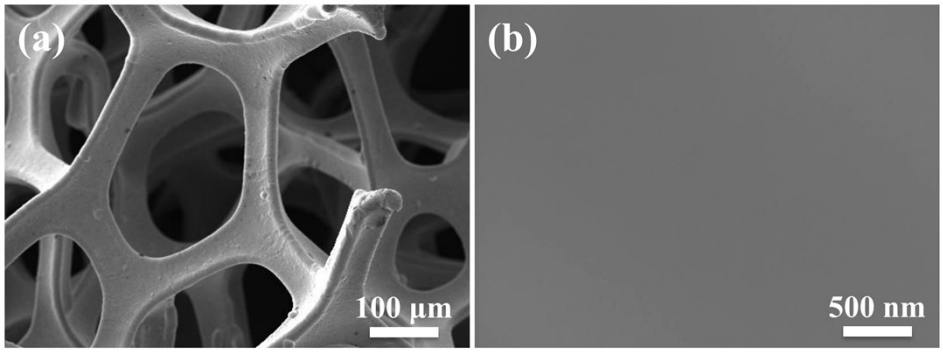

Figure S1 SEM images of bare Ni foam with different magnifications.

Figure S2 Time evolution images of thermal infusion molten Li process into bare Ni foam (conducted at a heating platform, 300 ℃).

Figure S3 Time evolution images of thermal infusion molten Li process into Au/NNS-NF (conducted at a heating platform, 300 ℃).

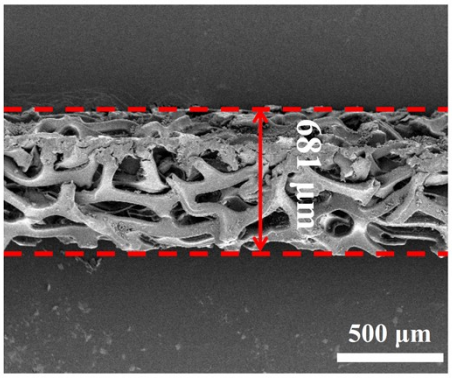

Figure S4 Cross-section SEM image of Au/NNS-NF

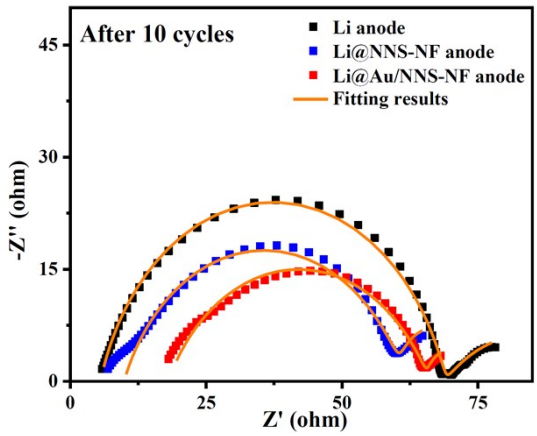

Figure S5 Nyquist plots of Li@Au/NNS-NF, Li@NNS-NF or bare Li based symmetric cells after 10 cycles.

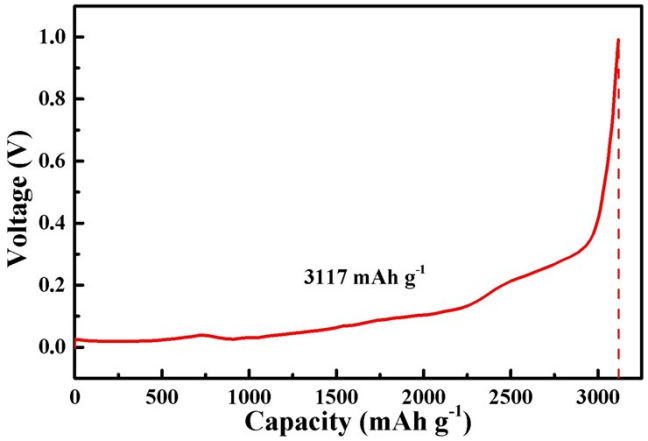

Figure S6 Li stripping curve of the Li@Au/NNS-NF electrode at a current density of 0.5 mA cm^{-2} with the cut-off voltage of 1.0 V.

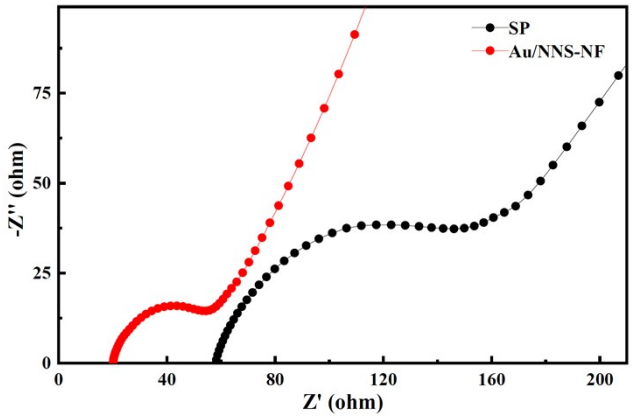

Figure S7 EIS spectra before cycling of the Li−O_2 batteries with the SP or Au/NNS-NF cathodes.

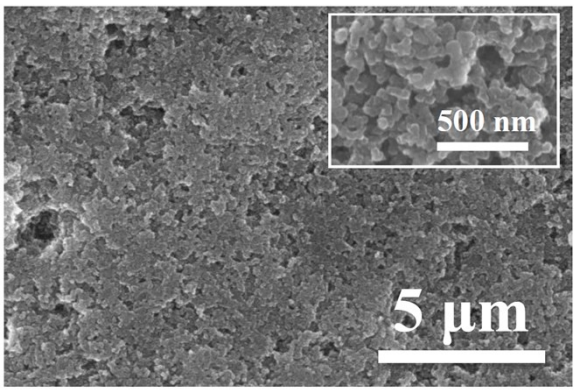

Figure S8 SEM images of the SP cathodes in Li−O_2 cells after discharge with the limited capacity of 1000 mAh g^{-1}.

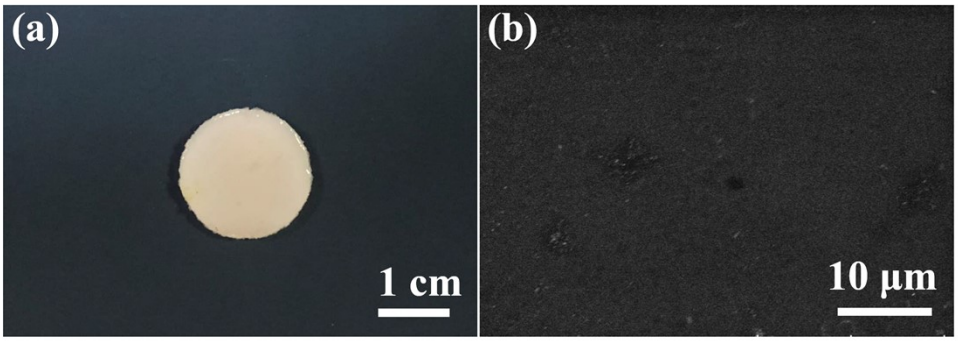

Figure S9 (a) Photographic and (b) SEM images of PMMA-based polymer electrolyte, respectively.

As shown in **Figure S9**, the as-prepared PMMA-based polymer electrolyte exhibits the typical solid-state morphology with no obvious pores in the bulk.

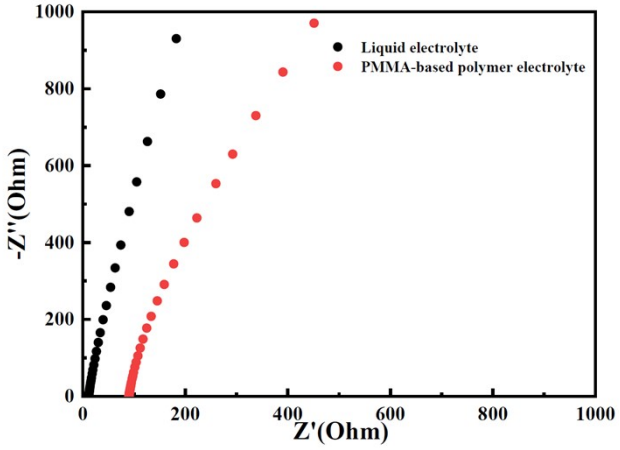

Figure S10 Nyquist plots of PMMA-based polymer electrolyte and liquid electrolyte.

Figure S10 gives the Nyquist plots of PMMA-based polymer electrolyte and liquid electrolyte. Electrochemical impedance spectroscopy of commercial celegard membrane with liquid electrolyte (thickness of 0.024 cm and area of 2.0 cm^2) and PMMA-based polymer electrolyte (thickness of 0.16 cm and area of 2.0 cm^2) in the frequency ranging from 0.01 Hz to 100 kHz using stainless steel sheets (SSS) symmetric cell (SSS/electrolyte/SSS).

It can be detected that the tested electrolyte resistances which are obtained from the intercept of the Nyquist plot with the real axis are ~11.5 and ~89.9 for conventional liquid electrolyte (1 M LiTFSI-TEGDME solution) and PMMA-based polymer electrolyte, respectively. The conductivity σ of the prepared electrolyte is obtained using the following equation:

$$\sigma = l/RS$$

Hence, σ for PMMA-based polymer electrolyte and liquid electrolyte can be calculated as 0.89 mS cm^{-1} and 1.04 mS cm^{-1}, respectively.

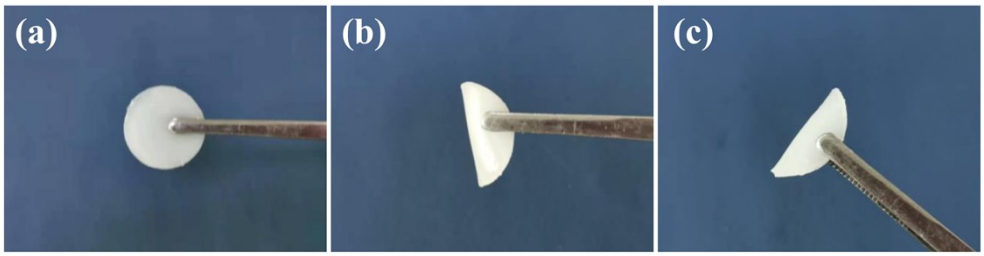

Figure S11 Toughness test, the tweezer is used to bend the PMMA-based polymer electrolyte film.

As shown in **Figure S11**, the PMMA-based polymer electrolyte film exhibits superior flexibility and high mechanical strength. It can be bent at different shapes without any structural damage.

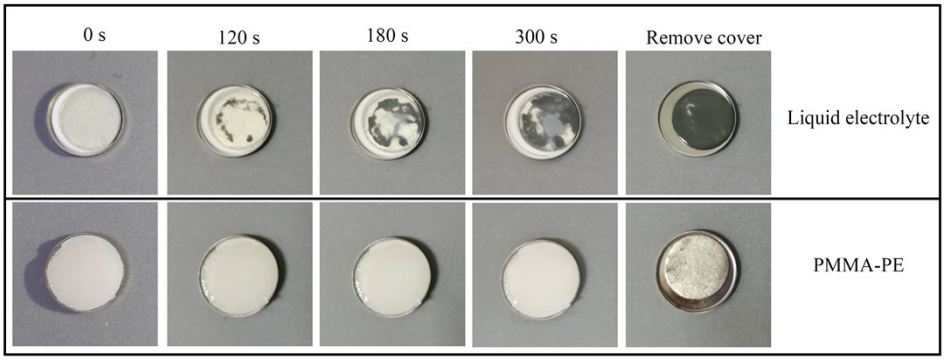

Figure S12 Surface morphology evolution of Li anodes that are protected with liquid electrolyte-immersed membrane or PMMA-based polymer electrolyte exposed to the ambient air.

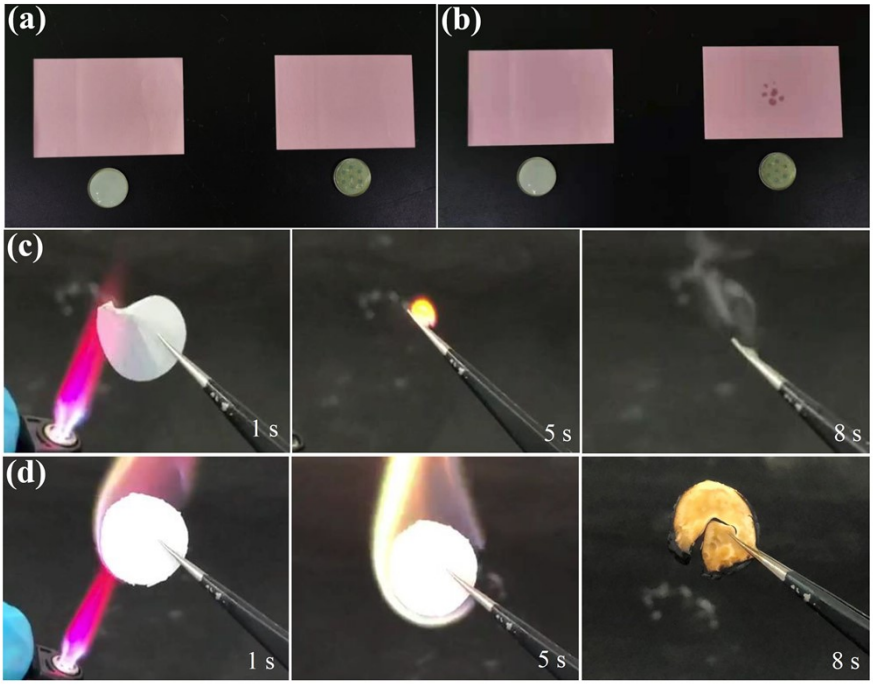

Figure S13 (a) Leakage test: PMMA-based polymer electrolyte-based battery case and (b) liquid electrolyte-based battery case before and after pressing on a piece of dry paper. And the combustion test of (c) 1 M LiTFSI-TEGDME based Celgard membrane and (d) PMMA-based polymer electrolyte.

As shown in Figure S13a-b, after pressing tightly on a piece of paper, PMMA-based polymer electrolyte does not make the paper wet but liquid electrolyte-based battery makes the paper wet. From the results of the combustion test (**Figure S13c-d**), the Celgard membrane with 1 M LiTFSI-TEGDME immediately burned once exposed to the flame. However, the PMMA-based polymer electrolyte can still keep its basic morphology even though exposed to a flame for several seconds. The above results suggest that PMMA-based polymer electrolyte has the good thermal stability and high safety.

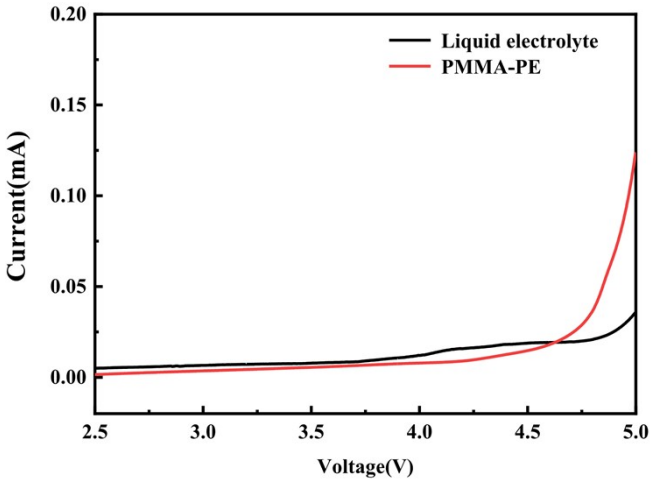

Figure S14 LSV for PMMA-based polymer electrolyte or liquid electrolyte at the sweep rate of 1 mV s^{-1}.

As shown in **Figure S14**, the main decomposition of PMMA-based polymer electrolyte begins at ~4.7 V (*vs.* Li^+/Li), which is similar to that of liquid electrolyte.

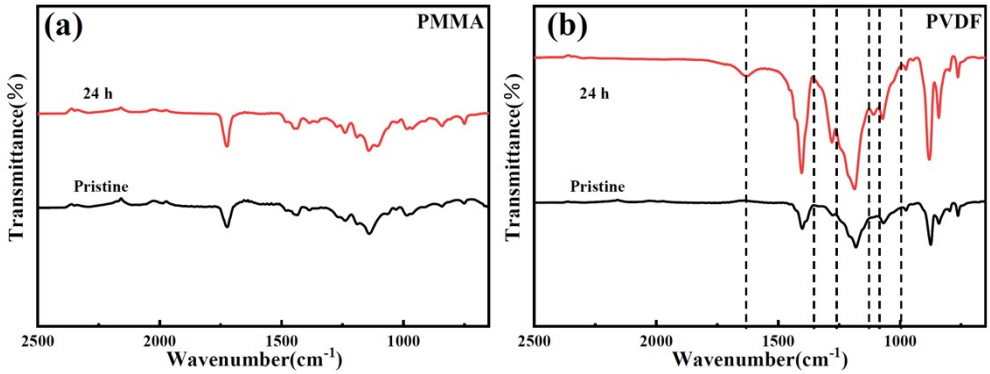

Figure S15 FT-IR spectra of (a) the pristine PMMA or (b) PVDF and the corresponding products obtained from (a) the reacted PMMA or (b) PVDF mixed with (KO_2+18-crown-6 in TEGDME) after 24 h.

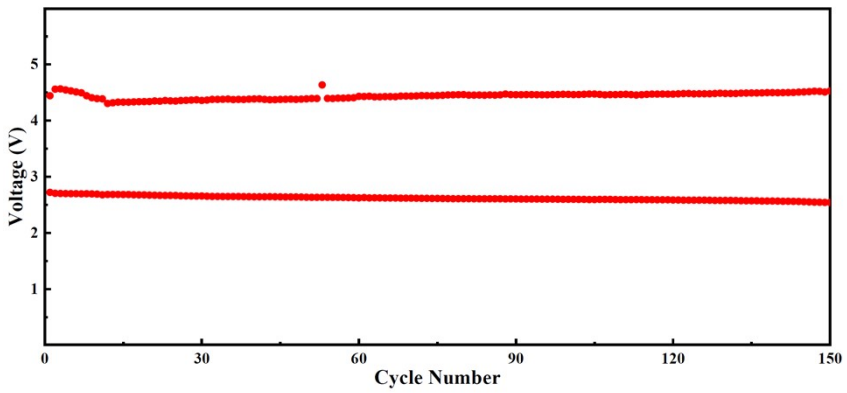

Figure S16 The corresponding discharge/charge terminal potentials vs cycling numbers of the quasi-symmetric Au/NNS-NF-based polymer Li–air cell.

Table S1 Comparison of electrochemical performances for Li-based anodes.

Materials	Component Electrolytes	Current Density	Overpotential (mV)	Cycle Time (h)	References
$Li_{4.4}Sn$/SG	1.0 M LiTFSI in DOL and DME	1 mA cm^{-2} (1 mAh cm^{-2})	34	600	Ref.S1
Li@MCI	1.0 M LiTFSI in DOL and DME with 2 % $LiNO_3$	1 mA cm^{-2} (1 mAh cm^{-2})	30	1500	Ref.S2
LiF@Po–Li	1.3 M $LiPF_6$ in EC: DEC =3:7 with 5% FEC	1 mA cm^{-2} (1 mAh cm^{-2})	40	1000	Ref.S3
Li/Mo	1.0 M LiTFSI in DOL and DME with 1 % $LiNO_3$	1 mA cm^{-2} (1 mAh cm^{-2})	20	1200	Ref.S4
sa-Li	1.0 M LiTFSI in DOL and DME	1 mA cm^{-2} (1 mAh cm^{-2})	28	1000	Ref.S5
TiC/C/Li	1.0 M LiTFSI in DOL and DME with 1 wt % $LiNO_3$	1 mA cm^{-2} (1 mAh cm^{-2})	42	400	Ref.S6
Li-Zn@NC@CC	1.0 M LiTFSI in DOL and DME with 2 wt % $LiNO_3$	1 mA cm^{-2} (1 mAh cm^{-2})	28	1200	Ref.S7
TiC/C/Li	1.0 M LiTFSI in DOL and DME with 1 wt % $LiNO_3$	1 mA cm^{-2} (1 mAh cm^{-2})	42	400	Ref.S8
Li-CF	1.0 M $LiPF_6$ in EC: DEC =1:1	1 mA cm^{-2} (1 mAh cm^{-2})	60	744	Ref.S9
HCT/Li	1.0 M LiTFSI in DOL and DME with 2 wt % $LiNO_3$	2 mA cm^{-2} (1 mAh cm^{-2})	100	500	Ref.S10
Li-cMOFs	1.0 M $LiPF_6$ in EC: DEC : MDC=1:1:1	1 mA cm^{-2} (1 mAh cm^{-2})	52	700	Ref.S11
Li-Ni@NiO-400	1.0 M $LiPF_6$ in EC: DEC : MDC=1:1:1 with 10% FEC	1 mA cm^{-2} (1 mAh cm^{-2})	26	2010	Ref.S12
Li@Au/NNS-NF	**1.0 M LiTFSI in DOL and DME with 2 wt % $LiNO_3$**	**1 mA cm^{-2} (1 mAh cm^{-2})**	**20**	**2200**	**This work**

As shown in **Table S1**, the Li@Au/NNS-NF based symmetrical cell presents the stable voltage curves with low average overpotentials of ~20 mV over long-term cycling (2200 h), which is much better than most of the previously reported Li-based electrodes (**Ref. S1-12**).

Table S2 Summary of the detailed resistance compositions of the Li@Au/NNS-NF, Li@NNS-NF or Li based symmetrical cells.

	R_e (Ω)	R_f (Ω)	R_{ct} (Ω)
Li anode	10.29	426.4	76.7
Li@NNS-NF anode	4.061	182	150
Li@Au/NNS-NF anode	17.94	104.1	72.28

Table S2 has further summarized the detailed resistance compositions of these symmetrical cells with Li@Au/NNS-NF, Li@NNS-NF and Li electrodes before cycling, in which R_e represents electrolyte resistance, while R_f and R_{ct} are corresponding to the SEI film and charging transfer resistances, respectively (the interface resistance is the sum of R_f and R_{ct}). It can be found from **Table S2** that the interfacial resistance of the Li@Au/NNS-NF based battery is only 176.38 Ω, which is smaller than these of the Li@NNS-NF (332 Ω) or Li (503.1 Ω) based symmetric cells before cycling.

Table S3 Summary of the detailed resistance compositions of the Li@Au/NNS-NF, Li@NNS-NF or Li based symmetrical cells after 10 cycles.

	R_e (Ω)	R_f (Ω)	R_{ct} (Ω)
Li anode	5.57	63.39	30.1
Li@NNS-NF anode	9.9	51.5	12.6
Li@Au/NNS-NF anode	18	48	8

After 10 cycles, the interfacial resistances of the bare Li and Li@NNS-NF electrodes rapidly decrease to 93.49 and 64.1 Ω, respectively, while the Li@Au/NNS-NF anode shows the smallest interfacial resistance variation rate over three Li-based anodes.

Table S4 Comparison of cycling performances for Li–air batteries.

Materials	Cycle Current (Capacity)	Overpotential (V)	Cycle Performance	References
Li-HDHPC	500 mA g^{-1} (1000 mAh g^{-1})	2.0	110	Ref.S13
phosphorene-coated Li	500 mA g^{-1} (1000 mAh g^{-1})	1.6	50	Ref.S14
SHCPE-Li	200 mA g^{-1} (500 mAh g^{-1})	2.5	95	Ref.S15
BA-Li	300 mA g^{-1} (1000 mAh g^{-1})	2.5	146	Ref.S16
gel-CLA-DCs	500 mA g^{-1} (500 mAh g^{-1})	2.0	100	Ref.S17
TLi	500 mA g^{-1} (1000 mAh g^{-1})	2.0	65	Ref.S18
Li@Au/NNS-NF	**500 mA g^{-1} (1000 mAh g^{-1})**	**<2**	**150**	**This work**

From **Table S4**, this the quasi-symmetric Au/NNS-NF-based polymer Li–air cell can keep the stable voltage profiles over 150 cycles, which is much better than most of these reported Li–air batteries (**Ref. S13-18**).

References

ref. S1: Y. Jiang, J. Jiang, Z. Wang, M. Han, X. Liu, J. Yi, B. Zhao, X. Sun, J. Zhang, *Nano Energy* **2020**, 70, 104504.

ref. S2: Z. Luo, S. Li, L. Yang, Y. Tian, L. Xu, G. Zou, H. Hou, W. Wei, L. Chen, X. Ji, *Nano Energy* **2021**, 87, 106212.

ref. S3: S. Sun, S. Myung, G. Kim, D. Lee, H. Son, M. Jang, E. Park, B. Son, Y.-G. Jung, U. Paik, T. Song, *J. Mater. Chem. A* **2020**, 8, 17229-17237.

ref. S4: J. Zhang, Q. Li, Y. Zeng, Z. Tang, D. Sun, D. Huang, Z. Peng, Y. Tang, H. Wang, *Chem. Eng. J.* **2021**, 426, 131110.

ref. S5: T. Xu, P. Gao, P. Li, K. Xia, N. Han, J. Deng, Y. Li, J. Lu, *Adv. Energy Mater.* **2020**, 10, 1902343.

ref. S6: Y. Cheng, R. Lu, K. Amin, B. Zhang, Q. Zhou, C. Li, L. Mao, Z. Zhang, X. Lu, Z. Wei, *ACS Appl. Energy Mater.* **2021**, 4, 6106-6115.

ref. S7: L. You, S. Ju, J. Liu, G. Xia, Z. Guo, X. Yu, *J. Energy Chem.* **2022**, 65, 439-447.

ref. S8: S. Liu, X. Xia, Y. Zhong, S. Deng, Z. Yao, L. Zhang, X.-B. Cheng, X. Wang, Q. Zhang, J. Tu, *Adv. Energy Mater.* **2018**, 8, 1702322.

ref. S9: Y. Zhang, C. Wang, G. Pastel, Y. Kuang, H. Xie, Y. Li, B. Liu, W. Luo, C. Chen, L. Hu, *Adv. Energy Mater*. **2018**, 8, 1800635.

ref. S10: M. Cheng, H. Su, P. Xiong, X. Zhao, Y. Xu, *ACS Appl. Energy Mater.* **2019**, 2, 8303-8309.

ref. S11: M. Zhu, B. Li, S. Li, Z. Du, Y. Gong, S. Yang, *Adv. Energy Mater.* **2018**, 8,

1703505.

ref. S12: G. Li, S. Xu, B. Li, T. Xia, J. Yu, F. Shao, Z. Yang, Y. Su, Y. Zhang, J. Ma, N. Hu, *J. Power Sources* **2021**, 506, 230161.

ref. S13: C. Li, J. Wei, K. Qiu, Y. Wang, *ACS Appl. Mater. Interfaces* **2020**, 12, 23010-23016.

ref. S14: Y. Kim, D. Koo, S. Ha, S. C. Jung, T. Yim, H. Kim, S. K. Oh, D. M. Kim, A. Choi, Y. Kang, K. H. Ryu, M. Jang, Y. K. Han, S. M. Oh, K. T. Lee, *ACS Nano* **2018**, 12, 4419-4430.

ref. S15: T. Liu, X. L. Feng, X. Jin, M. Z. Shao, Y. T. Su, Y. Zhang, X. B. Zhang, *Angew. Chem. Int. Ed.* **2019**, 58, 18240-18245.

ref. S16: Z. Huang, J. Ren, W. Zhang, M. Xie, Y. Li, D. Sun, Y. Shen, Y. Huang, *Adv. Mater.* **2018**, 30, e1803270.

ref. S17: J. Li, Z. Wang, L. Yang, Y. Liu, Y. Xing, S. Zhang, H. Xu, *ACS Appl. Mater. Interfaces* **2021**, 13, 18627-18637.

ref. S18: X. Zhang, Q. Zhang, X. G. Wang, C. Wang, Y. N. Chen, Z. Xie, Z. Zhou, *Angew. Chem. Int. Ed.* **2018**, 57, 12814-12818.